ADVANCED FUNCTIONAL MATERIALS
www.afm-journal.de

Highly Fluorescent and Color-Tunable Exciplex Emission from Poly(*N*-vinylcarbazole) Film Containing Nanostructured Supramolecular Acceptors

*Jong H. Kim, Byeong-Kwan An, Seong-Jun Yoon, Sang Kyu Park, Ji Eon Kwon, Chang-Keun Lim, and Soo Young Park**

Highly fluorescent excited-state charge-transfer complexes (exciplexes) formed at the interfacial region between a polymeric donor matrix, here, poly(*N*-vinylcarbazole), and embedded nanostructured acceptors are characterized for their photophysical properties. Exciplex-to-exciton emission switching is observed after solvent vapor annealing (SVA) due to the size evolution of the nanostructures beyond the exciton diffusion length. Color-tunable exiplex emission (sky blue, green, and orange) is demonstrated for three different nanostructured acceptors with the same HOMO–LUMO gap (i.e., the same blue excitonic emission) but with different electron affinity. White-emitting poly(*N*-vinylcarbazole) film is also fabricated, simply by incorporating mixed supramolecular acceptors, which provide independent exciplex emissions. This study presents important insights into the excited-state intermolecular interaction at the well-defined nanoscale interface and suggests an efficient way to obtain multicolored exciplex emissions.

1. Introduction

Specific intermolecular interactions in a bimolecular electron donor (D)–acceptor (A) system have been broadly investigated and their versatile applications in optoelectronic devices have been extensively studied.[1] It is well known that D–A systems can generate either charge-transfer (CT) complexes in the electronic ground state, or excited-state CT complexes (exciplexes) after one of the components is photoexcited.[1,2] In particular, exciplex formation, occurring between the excited singlet state of one molecule and the ground state of the other molecule, has attracted much attention due to its unique potential in tailoring emission wavelengths without altering the original absorption characteristics of the D–A pair.[3] Unfortunately, however, exciplex emission suffers from rather low photoluminescence (PL) quantum yields, since most exciplex species preferentially decay via nonradiative pathways due to increased intermolecular phonon interactions combined with an overall reduction in the oscillator strength of dimeric species[1c,4] and, what is worse, due to the current lack of molecules exhibiting high PL efficiency (particularly in the solid state), only a few studies of highly luminescent exciplex films have been reported so far.[1g] Thus, the tailored fine-tuning of emission wavelengths and also the prevention of fluorescence quenching using highly luminescent materials in the condensed state have been two essential issues and challenging tasks that need to be achieved for the practical optoelectronic application of exciplex emission.

We have been actively involved in the rational design of highly fluorescent and self-assembling molecular acceptors in the solid state, which form supramolecular nanoarchitectures with controllable size and morphology (nanoparticles, nanowires, nanofabrics, and coaxial nanocables).[5a-e] Recently, we have focused on their intermolecular stacking and D–A interactions for various optoelectronic applications.[5f-j]

Nanostructures based on this unique class of acceptor molecules feature tight intermolecular stacking and strong fluorescence emission.[5] It has been demonstrated that their hierarchical assembly into various dimensionalities could be directed by adjusting the molecular structural units (stilbenic compounds with cyano (–CN) and trifluoromethyl ($-CF_3$) substituents), which are important elements not only for self-assembly into nanostructures but also for lowering frontier molecular energy levels to meet the requirements of the acceptors in this work.[5e,h,6]

Herein, we take full advantage of the unique optoelectronic and structural benefits of these peculiar nanostructures as electron acceptors to suggest a novel and simple approach to obtain color-tunable supramolecular exciplexes (in particular, white emission from energy transfer-avoided blend films), featuring

Dr. J. H. Kim, Dr. S.-J. Yoon, S. K. Park, J. E. Kwon, Prof. S. Y. Park
Center for Supramolecular Optoelectronic Materials
Department of Materials Science and Engineering
Seoul National University
1 Gwanak-ro, Gwanak-gu, Seoul, 151-744, South Korea
E-mail: parksy@snu.ac.kr
Prof. B.-K. An
Department of Chemistry
The Catholic University of Korea
Wonmi-gu, Bucheon-si, Gyeonggi-do, 420-743, South Korea
Dr. C.-K. Lim
Biomedical Science Center, Korea Institute of Science and Technology
39-1, Hawolgok-dong, Seongbuk-gu, Seoul, 136-791, South Korea

DOI: 10.1002/adfm.201302924

a high fluorescence efficiency in the film state. Furthermore, exciplex/exciton color switching depending on the evolution of supramolecular nanostructures at the nanoscale interface is demonstrated.

2. Results and Discussion

The molecules used in this work as electron acceptors are 1-cyano-*trans*-1,2-bis-(4′-methylbiphenyl)ethylene) (CN-MBE, **1**),[5a] 1-cyano-*trans*-1,2-bis-(3′,5′-bis-trifluoromethyl-biphenyl) ethylene (CN-TFMBE, **2**),[5b] and 3,3′-(1,4-phenylene)bis(2-(3,5-bis(trifluoromethyl)phenyl)acrylonitrile (CN-TFPA, **3**),[5e] as shown in **Figure 1**a. These three molecules are selected in this work because they show the identical emission color (i.e., the same value of the highest occupied molecular orbital (HOMO)–lowest unoccupied molecular orbital (LUMO) gap), while having different electron affinity values to vary their CT interaction with a given electron donor polymer. All molecules were synthesized according to our previously published route.[5] Electron donor polymers poly(*N*-vinylcarbazole) (PVK) and poly[2-methoxy-5-(2′-ethylhexyloxy)-*p*-phenylene vinylene] (MEH-PPV), and also the electronically inactive poly(methyl methacrylate) (PMMA), were purchased from Sigma-Aldrich.

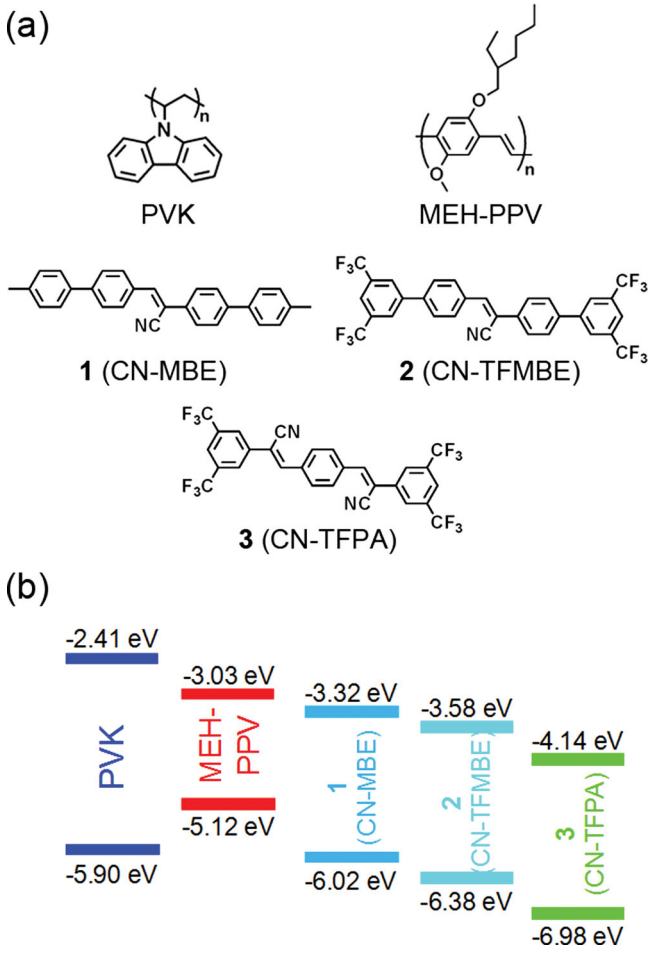

Figure 1. a) Chemical structures of polymer donors and supramolecular acceptors. b) Energy level diagram showing the HOMO and LUMO energy levels of the materials.

We first carried out quantum chemical calculations based on the density functional theory (DFT) to investigate the effect of specific electron-withdrawing units (–CF_3 and –CN) within the molecules on their frontier energy levels. It was found that LUMO energy levels of acceptors were lowered in the order of increasing strength of electron-withdrawing units, as shown in Table S1 of the Supporting Information. These results were evidenced by experimentally observing LUMO energy levels in the film state (see Figure 1b), which were obtained from HOMO energy levels (measured using ultraviolet photoelectron spectroscopy (UPS)), and optical bandgaps (E_g^{opt}) (shown as the UV–vis absorption onset).

Compounds **1**, **2**, and **3** showed virtually identical PL emission wavelengths (λ_{em}) peaking at 455, 453, and 450 nm (see **Figure 2**), respectively, when acceptors with 15 wt% to PVK concentration were embedded in electronically inactive PMMA films (excitation wavelengths (λ_{ex}) were 355, 340, and 353 nm, respectively, and UV–vis absorption spectra are shown in Figure S1). The electron-rich and hole-transporting polymer, PVK, which has excellent film-forming properties,[7] was used as an electron-donating matrix to induce excited-state interactions with the electron-deficient supramolecular acceptors in this study ($\lambda_{em,PVK}$ = 408 nm). As expected, emission wavelengths of all three acceptors exhibited remarkable shifts in PVK films compared with those in PMMA. Figure 2 clearly demonstrates that acceptor-embedded PVK (denoted as PVK/acceptor) films show red-shifted PL emissions with respect to those of PMMA films embedded with the same acceptors (PMMA/acceptor); emission wavelengths of **1**, **2**, and **3** were 478, 515, and 591 nm, respectively in PVK (excitation wavelengths (λ_{ex}) were 355, 340, and 353 nm, respectively). However, when the concentration of acceptors were increased over 30 wt% of PVK, exciplex emission was gradually decreased, while the excitonic emission of the acceptors was increased, as shown in Figure S2. A higher concentration of acceptors in PVK/acceptor brings about the increased size of acceptor domains beyond that of the exciton diffusion length in the blend film, which results in gradual emission changes from exciplex to exciton, as observed also in the SVA-treated PVK/acceptor films discussed later.

It should be noted that the absorption spectra of these acceptor-embedded PVK films are simple sum of those of PVK and supramolecular acceptors, as shown in Figure S1, and no new absorption bands are observed, ruling out any ground-state CT interactions. These results are clearly in accord with the unique characteristics of exciplexes.[8]

It is well known that the energy of the exciplex emission ($h\nu_{em}$) is related to the frontier energy levels of the two components (donor and acceptor) comprising the complex, according to $h\nu_{em} \sim HOMO_{donor} - LUMO_{acceptor} + C$, where C is the empirical Coulombic binding energy of the electron and hole in the donor–acceptor ion pair of the exciplex.[9] Consistent with this equation, exciplex emission wavelengths of **1**, **2**, and **3** in PVK were effectively controlled by the energy differences (ΔE) between the LUMO energy levels of the acceptors and the HOMO energy levels of the donor (see Figure 1; energy levels of PVK in film state were measured using the same method as explained above). In other words, the smaller the ΔE values,

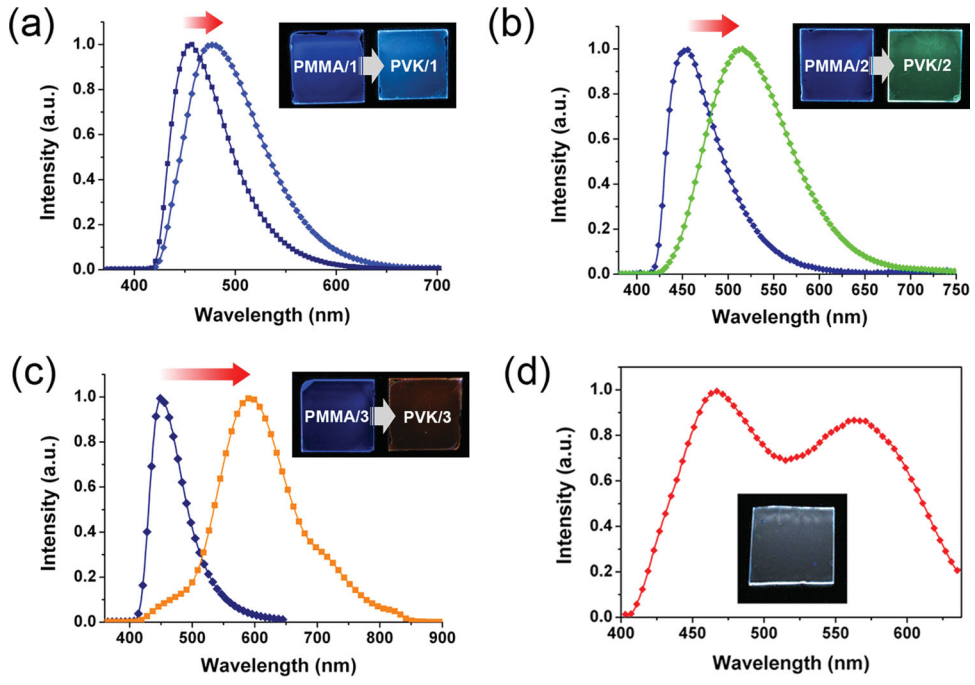

Figure 2. Normalized PL emission spectra of a) PMMA/**1** and PVK/**1**, b) PMMA/**2** and PVK/**2**, and c) PMMA/**3** and PVK/**3** films. d) Normalized PL spectrum of white fluorescent film prepared from blend solution of PVK/**1** and **3** (volume ration of **1** to **3** is 2:1) Insets images show emission wavelength changes of blend films (a–c) and white fluorescence (d) under 365 nm UV light.

the larger red-shift in the emission wavelength, due to the more stabilized complex formation. Corresponding to such energy level modification, we could easily obtain the sky blue (478 nm), green (515 nm), and orange (591 nm) emissions originating from the exciplexes formed at the interfaces of PVK and the nanostructured acceptors **1**, **2**, and **3**, respectively. The relationships between ΔE and emission shifts for the exciplex formation are summarized in **Table 1**.

For display or lighting applications, obtaining white light is attracting ever-increasing interest, most of which has been so far based on multilayer structures by the consecutive evaporation of two (or more) materials with different primary colors or, more conveniently, on spin-coated blends of soluble materials exhibiting different emissions.[10] Although the latter method is much more viable for practical applications, it is seriously restricted due to the extreme difficulty of emission color tuning related to the apparently unavoidable energy transfer crosstalk between different emitting species.[11] Herein, we demonstrate for the first time that the use of mixed supramolecular exciplexes provides white emission from spin-coating a single-layer polymer film free from any energy transfer cross talk.

Table 1. Information on the relationships between energy gap (ΔE) and emission shifts from exciplex formation ($\Delta\lambda$), average decay time of emission ($\tau_{em,avg}$) and absolute photoluminescence quantum yield (PLQY) of films.

Blend films	λ_{em} [nm][a)]	$\Delta\lambda_{em}$ [nm][b)]	ΔE [eV][c)]	$\tau_{em,avg}$ [ns][d)]	PLQY (Φ_{PL})[e)]
PMMA/1	455	–	–	1.2	–
PMMA/2	453	–	–	0.9	–
PMMA/3	450	–	–	0.3	–
PVK/1	478	23	2.58	3.2	0.39 (0.44)
PVK/2	515	62	2.32	48.2	0.22 (0.78)
PVK/3	591	141	1.76	45.8	0.09 (0.45)
PVK/1 and 3	468	–	–	1.2	0.11
	566			7.5	

[a)] λ_{em}: emission wavelength from blend film; [b)] $\Delta\lambda_{em}$: degree of emission wavelength-shift after exciplex formation; [c)] ΔE = $HOMO_{donor}$ – $LUMO_{acceptor}$; [d)] τ_{em}: average fluorescence lifetime; [e)] PLQY of pristine PVK film is 0.20 and values in parenthesis are PLQY of **1**, **2**, and **3** in bulk polycrystalline states, respectively.

Attributed to the efficient excited-state charge-transfer process (exciplex formation), we obtained a large Stokes shift of PVK/**3** (orange emission), which enabled us to avoid a spectral superposition between the absorption spectra of PVK/**3** and the emission spectra of PVK/**1** (sky blue emission), discouraging the energy transfer process, as shown in Figure 2 and S1. Moreover, the energy transfer to the exciplex species is inherently frustrated since their ground state population is only transient and thus depleted.[12] As a result, we could achieve real white emission with CIE coordinates of (0.33, 0.35), consisting of two exciplex emission peaks, by simply spin-coating a blend (PVK/**1** and **3**, volume ratio of compounds **1**:**3** is 2:1, and the PL spectrum of white emission is shown in Figure 2d). This result was possible due to the effective microphase segregation of supramolecular acceptors with their domain sizes smaller than the exciton diffusion length (see below for a more detailed discussion). Compared to the exciplex emission peaks of the individual PVK/**1** and PVK/**3**, those in three-compound blends (PVK/(**1** and **3**)) were slightly blue-shifted to 486 nm and 566 nm, respectively, most likely due to the partial miscibility of

1 and **3**, resulting in the modified energy levels of the exciplex emission. This approach to obtaining white emission by additive color mixing of two exciplex emissions is different from the previous exciplex-based white emission, which was achieved by the combined emissions from exciplex and exciton emission from the same component molecule.[12]

Moreover, despite the general observation that molecular exciplex emission is rather inefficient due to its lower transition dipole moment (from the singlet excited state to the ground state) compared to that of fluorescence,[13] exciplexes based on our supramolecular acceptors exhibited unexpectedly high absolute photoluminescence quantum yields (PLQY, Φ_{PL}) in films up to 0.39: higher than that of pristine PVK films (Table 1), presumably attributable to the interfacial nature of the exciplex and the high fluorescence efficiencies of the nanostructured acceptors in the condensed states.[5] Exciplex formation at the nanostructured interface was additionally evidenced from time-resolved PL decay measurements of blend films, as shown in **Figure 3**. The fluorescence lifetimes (τ_{em}) of PVK/acceptor films were drastically increased upon exciplex formation, compared to those of PMMA/acceptor films. The decay of PMMA/**1**, **2**, and **3** at λ_{em} of 455, 453, and 450 nm, respectively, is described by average lifetimes ($\tau_{em,avg}$s) of 1.2 ns, 893 ps and 328 ps, respectively. On the other hand, the delayed decay of PVK/**1**, **2** and **3** at red-shifted emission wavelengths of 478, 515, and 591 nm, respectively, is described by much longer $\tau_{em,avg}$s of 3.2, 48.2, and 45.8 ns, respectively, which is clearly attributed to the long-lived exciplexes (fluorescence lifetimes of all the measured blend films are summarized in Table 1 and Table S2).[8]

Such prevalent red-shifted exciplex emission with a delayed lifetime in the complete absence of excitonic emission is clear evidence that the generated excitons could effectively migrate to the intermolecular interfaces to form the exciplex, indicating that the size of nanostructured acceptors is still smaller than the exciton diffusion length.

In our previous work, gradual size growth of these nanostructured acceptors inside a variety of polymer matrices by solvent vapor annealing (SVA) was reported.[14] Based on this observation, we carried out SVA treatment of polymer blend films to explore the fluorescent emission changes as a function of the structural evolution of nanostructured acceptors. First, we exposed the PMMA/acceptor films, as a control, to dichloromethane (DCM) vapor to monitor the growth of self-assembled structures. With increasing SVA time, larger crystalline structures were formed, and accordingly the emissions at 455, 453, and 450 nm gradually red-shifted to those of bulk crystals at 472, 483, and 472 nm with $\tau_{em,avg}$s of 2.8, 6.7, and 3.6 ns (note that these were 1.2, 0.9, and 0.3 ns before SVA) at the vapor-exposed regions of PMMA/**1**, **2**, and **3** films, respectively (see Figure 3 and **Figure 4**d–f). When the same SVA treatments were applied to PVK/acceptor films, original exciplex emissions were gradually decreased, which accompanied increased excitonic emissions of bulk crystalline acceptors much like those in the PMMA film. After the growth of nanostructures over the size of the exciton diffusion length, exciplex emissions of the vapor-exposed regions were apparently switched to the their exciton emissions at 472, 483, and 472 nm with concomitantly decreased $\tau_{em,avg}$s of 2.7, 6.7, and

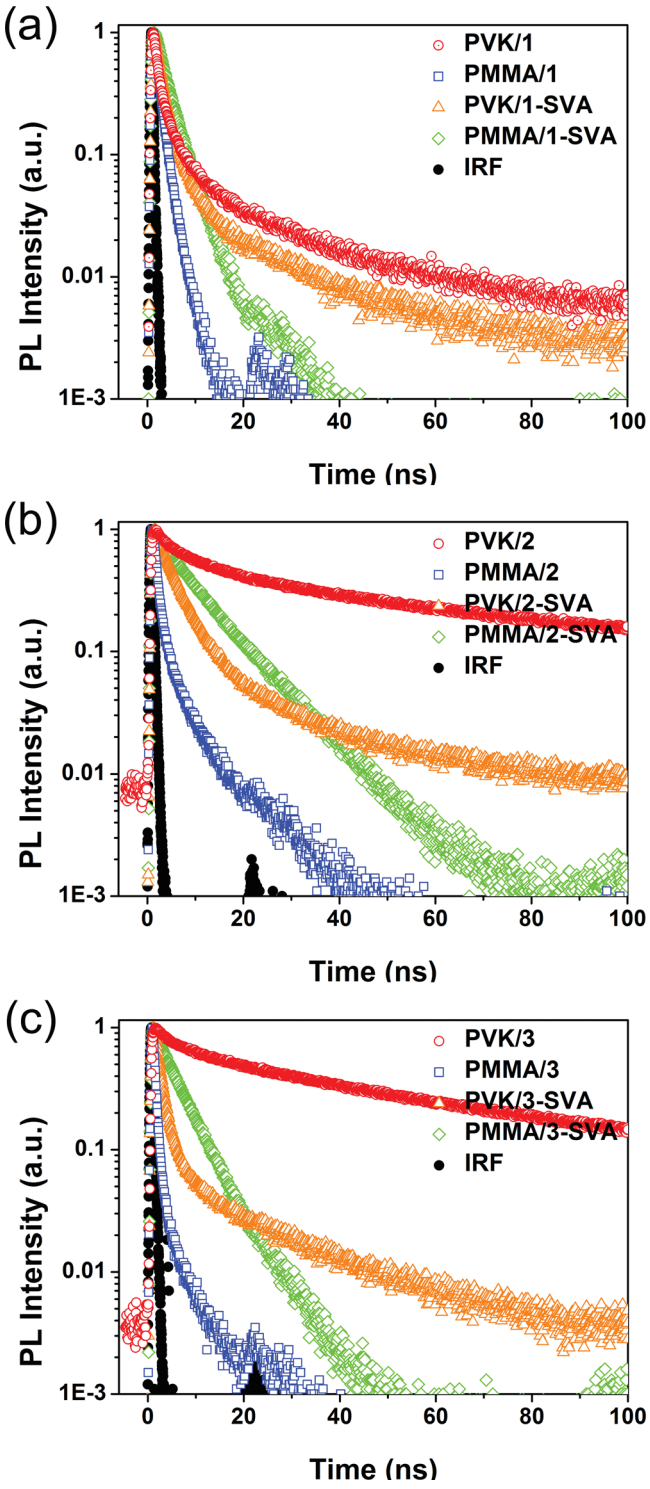

Figure 3. PL decay curves of a) **1**, b) **2**, and c) **3** embedded in PVK (open red circles), PMMA (blue squares) films with IRF (filled black circles) (open orange triangles and green diamonds representing PL decay curves of **1**, **2**, and **3** embedded PVK and PMMA films after solvent vapor annealing, respectively).

2.4 ns for **1**, **2**, and **3**, respectively (see Figure 3), which is due to the radiative decay of the exciton before it migrates through the bulk crystalline domains to the interface (PL spectral changes

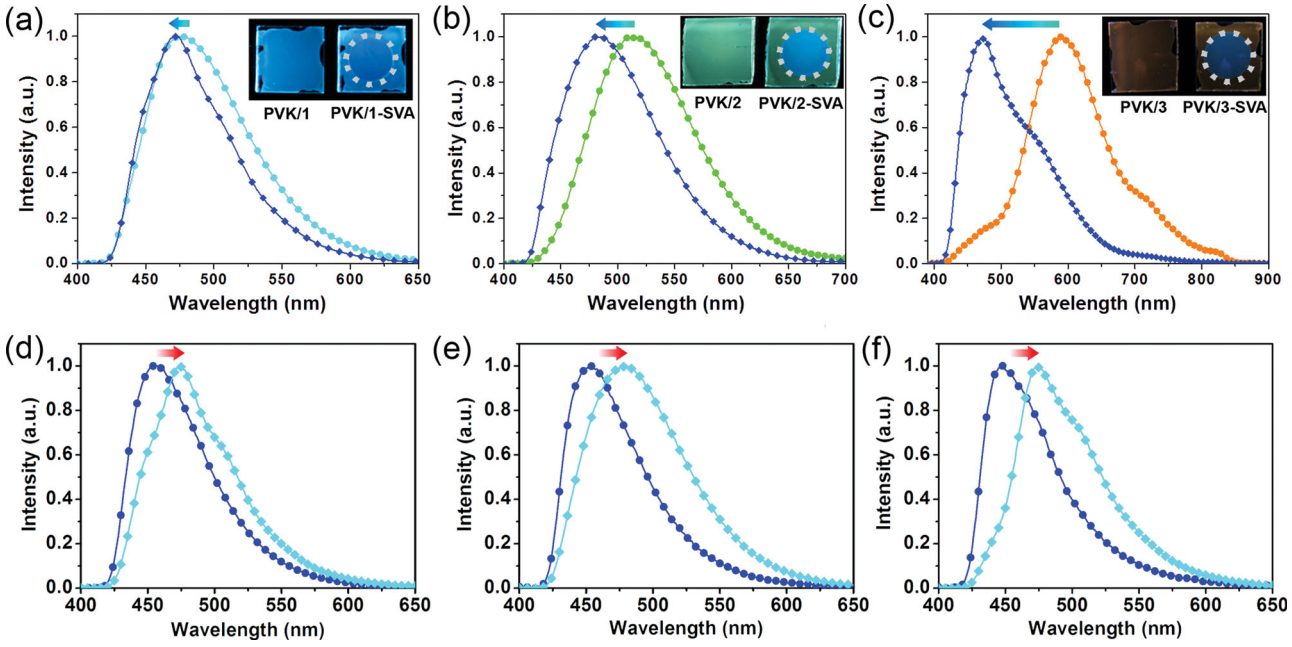

Figure 4. Changes in PL emission wavelengths of PVK/**1**, **2**, and **3** (a, b, and c), PMMA/**1**, **2**, and **3** (d, e, and f) films after solvent vapor annealing, respectively.

before and after the growth of the structures are shown in Figure 4a–c). It should be noted, however, that the emission spectrum of SVA films of PVK still comprise exciplex emission in part (although rather small), as seen in Figures 3 and 4. The structural evolution of **3** in PVK matrix and its emission change with SVA are schematically illustrated in **Figure 5**a. Fluorescence optical microscopy (FOM) images in Figure 5b and d more directly demonstrate the relationship between structural

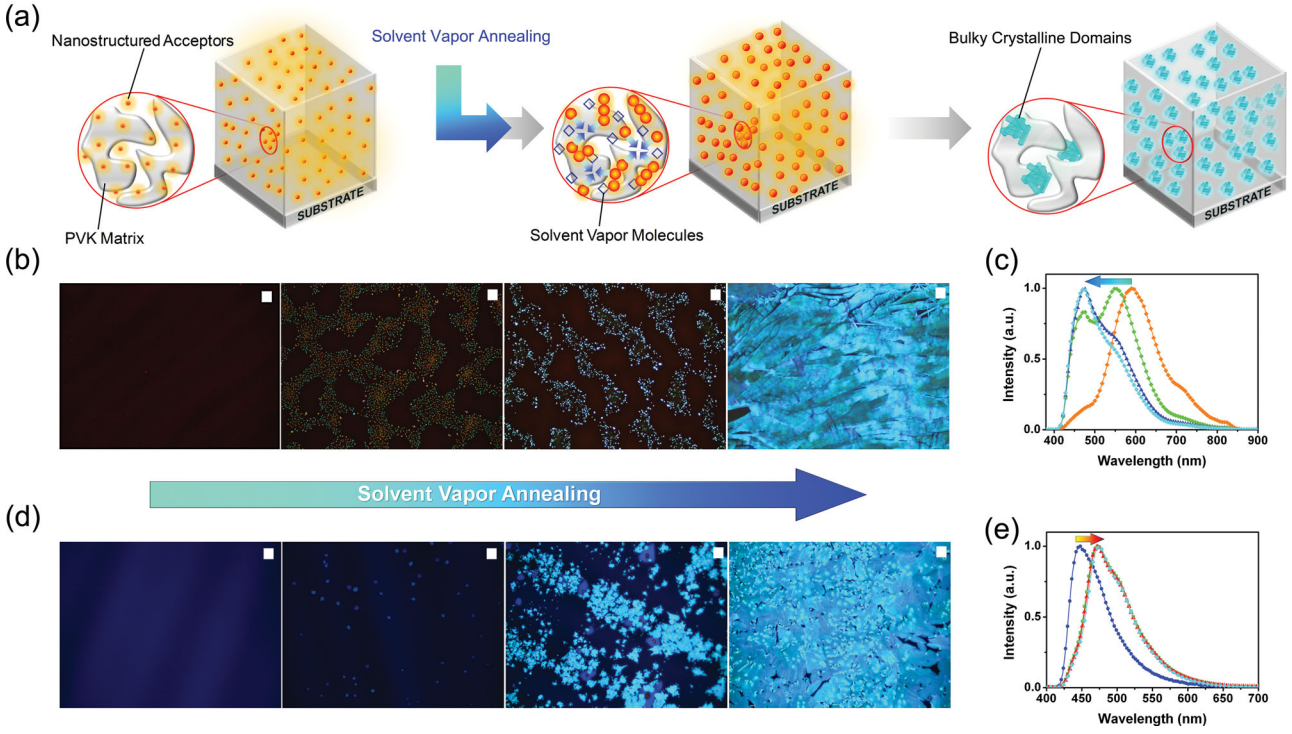

Figure 5. a) Schematic diagram of structural evolution of acceptor by solvent vapor annealing. Fluorescence optical microscopy images showing self-assembly-induced fluorescence changes of PVK/**3** (b) and PMMA/**3** (d) films, respectively, with solvent vapor annealing time (scale bar: 10 μm). PL emission spectra showing fluorescence changes of PVK/**3** (c) and PMMA/**3** (e) films, respectively, with solvent vapor annealing time, respectively.

evolution of **3** after SVA and the emission changes in PVK and PMMA. It is clearly shown that emissions from both matrices shifted and finally converged to the same fluorescence wavelength (472 nm) corresponding to that of a 2D bulk crystal of **3**, as shown in Figure 5c and e. In addition, $\tau_{em,avg}$s from PVK/**3** and PMMA/**3** films also converged after SVA treatment, as described in Table S2. To check any possible effect of SVA-treated PVK on exciplex-to-exciton emission switching, we compared optical and morphological changes of PVK films before and after SVA treatment. As shown in Figure S3, we could not find any changes in UV–vis absorption, PL emission spectra, or fluorescence lifetimes after SVA treatment (detailed information on fluorescence lifetime is given in Table S2). There was no morphological change to the PVK film after SVA either (see Figure S5). In addition, when we compared absorption spectra of PVK/acceptor blend before and after SVA, the modulated spectral region was limited only to that of the acceptor molecule, as shown in Figure S4.[14] Based on these observations, emission switching from exciplex to exciton was unambiguously attributed to the size evolution of the nanostructured acceptors.

For the quantitative evaluation of an effective domain size or distance (exciton diffusion length) of supramolecular acceptor to form the efficient exciplexes with PVK, we fabricated stacked bilayer films of PVK and supramolecular acceptors, rather than mixed ones. We grew nanostructures of **3** with controlled thicknesses through a vacuum thermal evaporation method on top of the PVK film. As shown in **Figure 6**a, 15 nm-thick films of **3** show orange exciplex emission (λ_{em} = 562 nm). For the >20 nm-thick films (see Figure 6b,c) of **3**, however, emission from the exciplex was largely suppressed and that from bulk crystalline domains (λ_{em} = 488 nm) appeared scanning electron microscope (SEM) images of morphologies of deposited compound **3** are shown in Figure S6). However, as expected, no significant fluorescence wavelength shift (no excited-state electronic interactions) was detected in the case where **3** was evaporated on PMMA films (reference samples), as shown in Figure 6d–f. From these measurements, the exciton diffusion length (L_D) of **3** could be estimated to be around 15 nm.

Measured fluorescence lifetimes of **3** (5.4 ns with 61.54% and 531 ps with 38.46%) enabled us to calculate the effective exciton diffusion length (L_D) value of **3** in the given nanostructure to compare with experimental value, according to $L_D^2 = D\tau_0$, where τ_0 is the dominant fluorescence lifetime (5.4 ns) and D is the exciton diffusion coefficient, which has been reported to have a value of 5.0×10^{-4} cm^2 s^{-1} for many conjugated organic materials.[15] We could obtain L_D of **3** as 16.4 nm, which is not only in the same range as the reported values of organic semiconductors[15] but also agrees well with the experimentally observed thickness where exciplex emission switches to that of exciton emission, with the evolution of the nanostructure in the stacked layers.

Interfacial exciplex emission is generally competing with the charge separation process, which gives rise to fluorescence quenching and photovoltaic currents. To explore the domain size effect of supramolecular acceptors for such applications other than exciplex emission, we have fabricated MEH-PPV films (see Figure 1 for the measured energy levels) with nanostructured acceptors **1**–**3**. When the supramolecular acceptors **1**, **2**, and **3** are embedded in MEH-PPV, different degrees of fluorescence quenching via photoinduced electron transfer, instead of exciplex emission, was observed. As shown in **Figure 7**, remarkable PL quenching (quenching efficiency of up to 99.4% accompanied by a faster PL decay, τ_{avg} of 25 ps) by charge-separation was

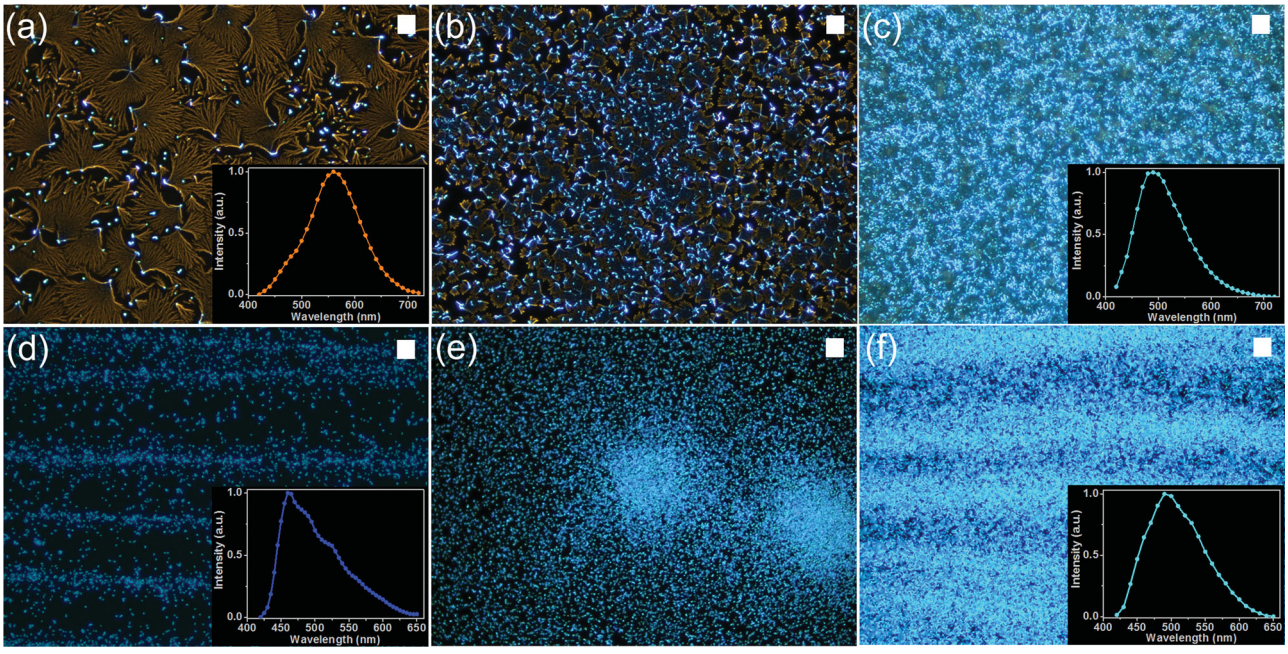

Figure 6. Fluorescence optical microscopy images of **3** evaporated on the PVK (a, b, and c), and PMMA (d, e, and f) films with different thicknesses of **3**, 15 (a,d), 20 (b,e), and 25 nm (c,f), respectively (scale bar: 10 μm, insets: PL emission spectra at each film).

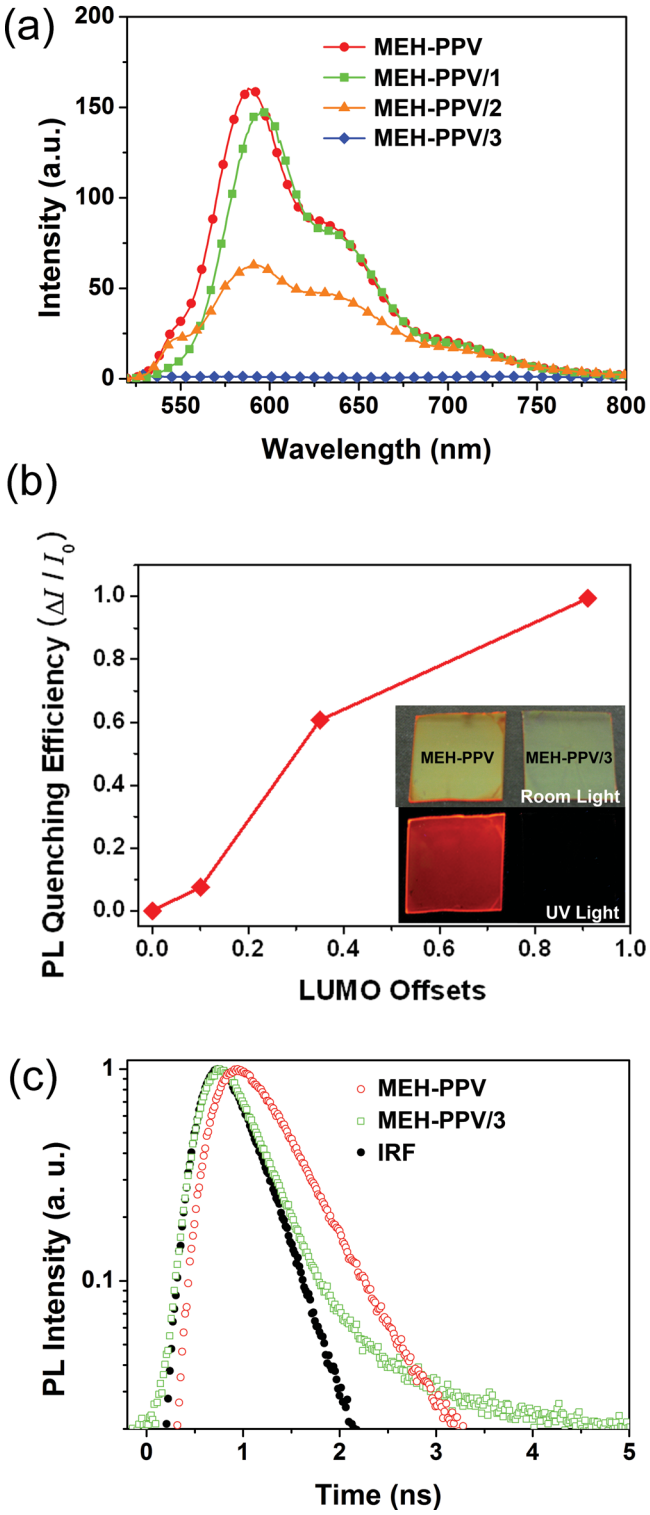

Figure 7. a) PL emission spectra of pristine MEH-PPV (red circles) and MEH-PPV/**1** (green squares), **2** (orange triangles), and **3** (blue diamonds) films. b) PL quenching efficiency of MEH-PPV/**3** (ΔI and I_0 are indicating the PL quenching and the PL intensity of the pristine MEH-PPV film, respectively, inset: images of pristine MEH-PPV and MEH-PPV/**3** films under room light and 365 nm UV light). c) PL decay curves of pristine MEH-PPV (open red circles), MEH-PPV/**3** (open green squares) films and IRF (filled black circles), respectively.

observed from MEH-PPV/**3** films. From the measurement of the photocurrent in bilayered photovoltaic cells comprising acceptor **3** stacked on top of donor MEH-PPV film under ambient conditions, we found that the short-circuit current (J_{SC}) and power-conversion efficiency (η_P) were optimized when the thickness of thermally deposited **3** was around the expected L_D (~15 nm) due to the optimized charge-separation efficiency at the interface. Over 20 nm-thick evaporation of **3**, however, performances of the devices decreased due to radiative excitonic decay before it reached the D–A interface (see Figure S7). Detailed results and information on the photophysical and electrical measurements are described in the Supporting Information.

3. Conclusions

We have provided a facile method to prepare highly efficient and color-tunable (sky blue, green, and orange) exciplexes by embedding highly fluorescent supramolecular acceptors into a polymeric donor (PVK). A white-emitting PVK film was also demonstrated from a simple mixture of supramolecular acceptors, which showed independent exciplex emissions without energy transfer. Furthermore, we presented exciplex-to-exciton emission switching due to the size evolution of the acceptors. Based on controlled LUMO energy levels and strong self-assembly of the nanostructures, the correlation between energy levels and excited-state processes, and the dependence of these processes at the well-defined nanoscale interface on exciton diffusion properties, were clearly investigated.

4. Experimental Section

Quantum Chemical Calculations: Single molecule calculations were conducted at the density functional theory (DFT) level of theory with the Gaussian 09 software.[16] The ground state geometry in the gas phase was fully optimized using the B3LYP functional and 6-31G** basis set.

Characterization: The UV–vis absorption and fluorescence emission spectra were recorded on a Shimadzu UV-1650 PC spectrometer and VARIAN Cary Eclipse spectrofluorophotometer, respectively. Time-resolved fluorescence lifetime experiments were performed by the time-correlated single photon counting (TCSPC) technique with a FluoTime200 spectrometer (PicoQuant) equipped with a PicoHarp300 TCSPC board (PicoQuant) and a PMA182 photomultiplier (PicoQuant). The excitation source was a 342 nm picosecond pulsed diode laser (PicoQuant, PLS340) driven by a PDL800-D driver (PicoQuant) with FWHM ~ 20 ps. The absolute photoluminescence quantum yield of the films was measured using an integrating sphere (Labsphere Co., 600 diameter). A continuous wave Xe-lamp (500 W, Melles Griot Co.) was used as the excitation source, and a monochromator (Acton Research Co.) attached to a photomultiplier tube (Hamamatsu) was used as the optical detector system. All of the systems were calibrated using a tungsten–halogen standard lamp and deuterium lamp (Ocean Optics LS-1-CAL and DH-2000-CAL, respectively). The photographs were obtained using a digital camera (Canon-PowerShot G6) and an optical microscope (Leica) under illumination at 365 nm. Fluorescence optical images and their photoluminescence spectrum were acquired with Nuance FX multispectral imaging system (Cambridge Research & Instrumentation). FE-SEM images were obtained using JEOL JSM-6330F and, prior to measurement, samples were coated with a 3-nm Pt layer to prevent charging. Current density–voltage (*J*–*V*) measurements were carried out under ambient conditions with a Keithley 4200 source measurement unit under AM 1.5G illumination at 100 mW cm^{-2} (Oriel SOL3A class AAA

solar simulator) with respect to a reference monocrystalline silicon cell certified at the National Renewable Energy Laboratory.

Preparation of Films and Solvent Vapor Annealing (SVA): 2.0 wt% solutions of small molecules (15 wt% with respect to PVK) and pristine PVK in 1,2-dichloroethane (DCE) were prepared. A white-emitting film was fabricated by spin-coating a mixture solution prepared from 2:1 volume ratio of PVK/**1** and PVK/**3** solutions. To compare emissions from exciplexes and those from small molecules, solutions of all small molecules with the same concentration were prepared for PMMA as well. 2.0 wt% solutions of small molecules (15 wt% with respect to MEH-PPV) and pristine MEH-PPV in *o*-dichlorobenzene were prepared to observe PL quenching. All small molecule (**1**, **2**, and **3**)-embedded thin films were fabricated by spin-coating (2500 rpm, 60 s) from the filtered solutions. For SVA treatment, the prepared films were then inverted and placed at the mouth of an 8 mL vial containing 1 mL DCM at room temperature.

Device Fabrication: Prior to device fabrication, ITO (160 nm, 10 Ω/υ) substrates were cleaned by sonication in trichloroetylene, acetone and isopropyl alcohol for 15 min each and subsequently dried in an oven for 3 h. The substrates were then exposed to UV light (360 nm) for 10 min. The cleaned substrates were carried into a nitrogen-filled glovebox, and PEDOT:PSS layer was spin-coated onto ITO surface. After baking at 120 °C for 1 h, MEH-PPV layer was spin-coated from the solution (1 wt% in *o*-dichlorobenzene) on the ITO/PEDOT:PSS substrates. After removing residual solvents by drying at 85 °C for 1 h, the film was transferred into a vacuum thermal evaporator in the same glovebox. CN-TFPA layer with different thicknesses was then deposited by thermal evaporation under the vacuum of 7×10^{-7} Torr at a deposition rate of 0.1–0.2 Å s^{-1}. Finally, aluminum electrode (100 nm) was deposited in sequence under the vacuum of 3×10^{-6} Torr at a deposition rate of 0.3–0.4 Å s^{-1}, using a shadow mask to define 0.3 cm × 0.3 cm device areas.

Supporting Information

Supporting Information is available from the Wiley Online Library or from the author.

Acknowledgements

This work was supported by the National Research Foundation of Korea (NRF) grant funded by the Korea government (MSIP) (No. 2009-0081571).

Received: August 20, 2013
Revised: November 6, 2013
Published online: January 16, 2014

[1] a) T. Noda, H. Ogawa, Y. Shirota, *Adv. Mater.* **1999**, *11*, 283; b) Y. Kawabe, J. Abe, *Appl. Phys. Lett.* **2002**, *81*, 493; c) C. Giebeler, H. Antoniadis, D. D. C. Bradley, Y. J. Shirota, *J. Appl. Phys.* **1999**, *85*, 608; d) J. Y. Kim, K. Lee, N. E. Coates, D. Moses, T.-Q. Nguyen, M. Dante, A. J. Heeger, *Science* **2007**, *317*, 222–225; e) F. Silvestri, M. D. Irwin, L. Beverina, A. Facchetti, G. A. Pagani, T. J. Marks, *J. Am. Chem. Soc.* **2008**, *130*, 17640; f) R. Qin, W. Li, C. Li, C. Du, C. Veit, H.-F. Schleiermacher, M. Andersson, Z. Bo, Z. Liu, O. Inganäs, U. Wuerfel, F. Zhang, *J. Am. Chem. Soc.* **2009**, *131*, 14612; g) S. L. Lai, M. Y. Chan, Q. X. Tong, M. K. Fung, P. F. Wang, C. S. Lee, S. T. Lee, *Appl. Phys. Lett.* **2008**, *93*, 143301.

[2] H. Aleves, A. S. Molinari, H. Xie, A. F. Morpurgo, *Nat. Mater.* **2008**, *7*, 574.

[3] a) K. Itano, H. Ogawa, Y. Shirota, *Appl. Phys. Lett.* **1998**, *72*, 636; b) J. A. Osaheni, S. A. Jenekhe, *Macromolecules*. **1994**, *27*, 739; c) C. J. Liang, W. C. H. Choy, *Appl. Phys. Lett.* **2006**, *89*, 251108.

[4] a) J. Wang, Y. Kawabe, S. E. Shaheen, M. M. Morrell, G. E. Jabbour, P. A. Lee, J. Anderson, N. R. Armstrong, B. Kippelen, E. A. Mash, N. Peyghambarian, *Adv. Mater.* **1998**, *10*, 230; b) M. Cocchi, D. Virgili, G. Giro, V. Fattori, P. D. Marco, J. Kalinowski, Y. Shirota, *Appl. Phys. Lett.*, **2002**, *80*, 2401; c) J. B. Birks, Photophysics of aromatic molecules, Wiley-Interscience, London, **1970**.

[5] a) B.–K. An, S.-K. Kwon, S.-D. Jung, S. Y. Park, *J. Am. Chem. Soc.* **2002**, *124*, 14410; b) B.-K. An, D.-S. Lee, J.-S. Lee, Y.-S. Park, H.-S. Song, S. Y. Park, *J. Am. Chem. Soc.* **2004**, *126*, 10232; c) B.-K. An, S. H. Gihm, J. W. Chung, C. R. Park, S.-K. Kwon, S. Y. Park, *J. Am. Chem. Soc.* **2009**, *131*, 3950; d) J. H. Kim, A. Watanabe, J. W. Chung, Y. Jung, B.-K. An, H. Tada, S. Y. Park, *J. Mater. Chem.* **2010**, *20*, 1062; e) S. K. Park, J. H. Kim, S.-J. Yoon, O. K. Kwon, B.-K. An, S. Y. Park, *Chem. Mater.* **2012**, *24*, 3263; f) S.-J. Yoon, J. W. Chung, J. Gierschner, K. S. Kim, M.-G. Choi, D. Kim, S. Y. Park, *J. Am. Chem. Soc.* **2010**, *132*, 13675; g) S.-J. Yoon, S. Varghese, S. K. Park, R. Wannemacher, J. Gierschner, S. Y. Park, *Adv. Opt. Mater.* **2013**, *1*, 232; h) S. K. Park, S. Varghese, J. H. Kim, S.-J. Kim, S.-J. Yoon, O. K. Kwon, B.-K. An, J. Gierschner, S. Y. Park, *J. Am. Chem. Soc.* **2013**, *135*, 4757; i) S. Kim, S.-J. Yoon, S. Y. Park, *J. Am. Chem. Soc.* **2012**, *134*, 12091; j) J. W. Chung, S.-J. Yoon, B.-K. An, S. Y. Park, *J. Phys. Chem. C* **2013**, *21*, 11285.

[6] J. H. Kim, J. W. Chung, Y. Jung, S.-J. Yoon, B.-K. An, H. S. Huh, S. W. Lee, S. Y. Park, *J. Mater. Chem.* **2010**, *20*, 10103.

[7] a) I. D. Parker, Q. Pei, M. Marrocco, *Appl. Phys. Lett.* **1994**, *65*, 1272; b) C. Zhang, H. von Seggern, K. Pakbaz, B. Kraabel, H.-W. Schmidt, A. J. Heeger, *Synth. Met.* **1994**, *62*, 35; c) C. Zhang, H. von Seggern, B. Kraabel, H.-W. Schmidt, A. J. Heeger, *Synth. Met.* **1995**, *72*, 185; d) G. E. Johnson, K. M. McGrane, M. Stolka, *Pure Appl. Chem.* **1995**, *67*, 175.

[8] a) A. C. Morteani, A. S. Dhoot, J.-S. Kim, C. Silva, N. C. Greenham, C. Murphy, E. Moons, S. Ciná, J. H. Burroughes, R. H. Friend, *Adv. Mater.* **2003**, *15*, 1708; b) A. C. Morteani, P. Sreearunothai, L. M. Herz, R. H. Friend, C. Silva, *Phys. Rev. Lett.* **2004**, *92*, 247402–247401; c) C. Dyer-Smith, J. J. Benson-Smith, D. D. C. Bradley, H. Murata, W. J. Mitchell, S. E. Shaheen, S. A. Haque, J. Nelson, *J. Phys. Chem. C* **2009**, *113*, 14533; d) J. J. Benson-Smith, J. Wilson, C. Dyer-Smith, K. Mouri, S. Yamaguchi, H. Murata, J. Nelson, *J. Phys. Chem. B* **2009**, *113*, 7794.

[9] N. J. Turro, Modern molecular photochemistry. University Science Books, Sausalito, California, **1991**.

[10] a) Z. Xie, J. S. Huang, C. N. Li, Y. Wang, Y. Q. Li, J. Shen, *Appl. Phys. Lett.* **1999**, *74*, 641; b) C. W. Ko, Y. T. Tao, *Appl. Phys. Lett.* **2001**, *79*, 4234; c) C.-H. Kim, J. Shinar, *Appl. Phys. Lett.* **2002**, *80*, 2782; d) M. Granström, O. Inganäs, *Appl. Phys. Lett.* **1996**, *68*, 147; e) S. Tasch, E. J. W. List, O. Ekström, W. Graupner, G. Leising, P. Schlichting, U. Rohr, Y. Geerts, U. Scherf, K. Müllen, *Appl. Phys. Lett.* **1997**, *71*, 2883.

[11] M. Anni, G. Gigli, V Paladini, R. Cingolani, G. Barbarella, L. Favaretto, G. Sotgiu, M. Zambianchi, *Appl. Phys. Lett.* **2000**, *77*, 2458.

[12] a) C.-I. Chao, S.-A. Chen, *Appl. Phys. Lett.* **1998**, *73*, 426; b) J. Thompson, R. I. R. Blyth, M. Mazzeo, M. Anni, R. Cingolani, *Appl. Phys. Lett.* **2001**, *79*, 560; c) M. Mazzeo, D. Pisignano, F. D. Sala, J. Thompson, R. I. R. Blyth, G. Gigli, R. Cingolani, G. Sotgiu, G. Barbarella, *Appl. Phys. Lett.* **2003**, *82*, 334.

[13] D. D. Gebler, Y. Z. Wang, D.-K. Fu, T. M. Swager, A. J. Epstein, *J. Chem. Phys.* **1998**, *108*, 7842.

[14] a) J. W. Chung, B.-K. An, F. Hirato, J. H. Kim, H. Jinnai, S. Y. Park, *J. Mater. Chem.* **2010**, *20*, 7715; b) B.-K. An, S.-K. Kwon, S. Y. Park, *Angew. Chem. Int. Ed.* **2007**, *46*, 1978.

[15] M. M. Alam, S. A. Jenekhe, *J. Phys. Chem. B* **2001**, *105*, 2479.

[16] M. J. Frisch et al., Gaussian 09, Revision A.02, Gaussian, INC., Wallingford, CT, **2009**.